16th Australasian Fluid Mechanics Conference
Crown Plaza, Gold Coast, Australia
2-7 December 2007

Numerical Simulation of Free-fountains in a Homogeneous Fluid

N. Srinarayana[1], S. W. Armfield[1] and W. X. Lin[2]

[1]School of Aerospace, Mechanical and Mechatronic Engineering
The University of Sydney, NSW, 2006 AUSTRALIA

[2]School of Engineering
James Cook University, QLD, 4811 AUSTRALIA

Abstract

The behaviour of plane fountains, resulting from the injection of dense fluid upwards into a large container of homogeneous fluid of lower density, is investigated. The transient behaviour of fountains with parabolic inlet velocity profile and Reynolds numbers, $50 \leq Re \leq 150$, Prandtl numbers, Pr=7, 300 and 700, and Froude numbers, $Fr = 0.25$ to 10.0 are studied numerically. The fountain behaviour falls into three distinct regimes; steady and symmetric; unsteady and periodic flapping; unsteady and aperiodic. The analytical scaling of non-dimensional fountain height, z_m, with Fr and Re is $z_m \sim Fr^{4/3-2\gamma/3}Re^{-\gamma}$. The constant γ is found empirically for each of the regimes. The fountain height decreases with increase in Reynolds number in the steady region but increases with Reynolds number in the unsteady regimes. However, the fountain height increases with Froude number in all regimes. Numerical results and the analytical scaling show that z_m is independent of Prandtl number in the range considered. The fountain exhibits periodic lateral oscillations, i.e., periodic flapping for intermediate Froude numbers ranging from $1.25 \leq Fr \leq 2.25$.

Introduction

A fountain is formed whenever a fluid is injected upwards into a lighter fluid, or downward into a denser fluid. In the former case the jet penetrates some distance and falls back as a plunging plume around the entering fluid.

Fountains are found in many engineering applications: the heating of a large open structure, such as an aircraft hanger, by large fan-driven heaters at the ceiling level; cooling of turbine blades; cooling of electronic components; the mixing of a two-layer water reservoir with propellers; and the mixing in metallurgical furnaces by gas bubble plumes, to name just a few. Hence it is important to understand the fundamental physics of such flows.

The behaviour of plane fountains is governed by the Reynolds, Froude, and Prandtl numbers, defined as,

$$\begin{aligned} Re &\equiv \frac{V_{in}X_{in}}{\nu}, \\ Fr &\equiv \frac{V_{in}}{\sqrt{g(\rho_{in}-\rho_\infty)/\rho_\infty X_{in}}} \\ &\equiv \frac{V_{in}}{\sqrt{g\beta(T_\infty - T_{in})X_{in}}}, \\ Pr &\equiv \frac{\nu}{\kappa}, \end{aligned} \tag{1}$$

where X_{in} and V_{in} are the half-width and velocity of a uniform inlet profile at the fountain source respectively, ν is the kinematic viscosity of the fountain fluid, g is the acceleration due to gravity, ρ_{in} and T_{in} are the density and temperature of the fountain fluid at the source respectively, ρ_∞ and T_∞ are the density and temperature of the ambient fluid respectively, κ is the thermal diffusivity and β is the coefficient of volumetric expansion. The second expression of the Froude number in equation (1) applies when the density difference is due to the difference in temperature of the fountain and ambient fluid using the Oberbeck–Boussinesq approximation.

Baines et al. [1] showed that if the source size is small compared with the fountain height for a plane turbulent fountain the flow will depend only on m_{in} and b_{in}, the inlet momentum and buoyancy fluxes per unit mass per unit span. Dimensional consistency then requires that the fountain height obeys the relation,

$$z_m = \frac{Z_m}{X_{in}} = \frac{C^* m_{in} b_{in}^{-2/3}}{X_{in}}, \tag{2}$$

where Z_m is the fountain height, z_m its non-dimensional form, $m_{in} = 2V_{in}^2 X_{in}$, $b_{in} = 2g(\rho_{in}-\rho_\infty)/\rho_\infty V_{in}X_{in}$ and C^* is a constant of proportionality. In terms of Fr z_m can be written as,

$$z_m = CFr^{4/3}, \tag{3}$$

where C is a constant of proportionality.

Baines et al. [1] then conducted a series of experiments on plane fountains to validate the scaling equation (2) for $500 \leq Fr \leq 3400$ and found that $C = 0.65$. However, Campbell and Turner [2] obtained C=1.64–1.97 from their experiments on plane turbulent fountains for $5.6 \leq Fr \leq 51$. Zhang and Baddour [3] conducted a series of experiments on plane turbulent fountains primararily to study the effect of mass flux, momentum flux and buoyancy flux on the properties of plane turbulent fountains for large and small Froude number, as the effect of mass flux on small Froude number fountains was not quantified in previous investigations. Two different models were used by them to correlate the small Froude number data and to quantify the effect of mass flux on plane fountains. The first model (virtual source model) applied the concept of virtual origin proposed by Morton [4] and the second model (zero-entrainment model) ignored the turbulent entrainment. The Froude number and the Reynolds number were in the ranges of $0.6 \leq Fr \leq 114$ and $325 \leq Re \leq 2700$ respectively. For $Fr < 6.5$, their virtual source model gave,

$$z_m = \left(2.0 - 1.12Fr^{-2/3}\right)Fr^{4/3}, \tag{4}$$

and their zero-entrainment model gave,

$$z_m = 0.71Fr^2. \tag{5}$$

Zhang and Baddour [3] used the scaling equation (3) for large Froude number experiments ($Fr \geq 10$) and obtained C=2.0, which is reasonably close to the range of values obtained by Campbell and Turner [2], but is about three times the value obtained by Baines et al. [1]. They speculated that Baines et al. [1] misinterpreted the value of C from Campbell and Turner [2] and probably miscalculated the equivalent half-width as even a small error in estimating the half-width could have a large effect on C. Their experimental results also showed that scaling equation (3) was reasonable over the entire range of Froude numbers investigated, whereas equation (4) was only adequate for $Fr < 4.0$.

Goldman and Jaluria [5] carried out an experimental investigation on plane fountains by blowing hot air vertically downward into a chamber which is different from the experiments discussed previously where salt solution was injected into a tank of fresh water. The Reynolds number and the Froude number were varied in the range $500 \leq Re \leq 2500$ and $1.4 \leq Fr \leq 15.8$ respectively. The fountain height was quantified by defining it as the vertical distance from the jet inflow to the location where the local temperature excess $(T - T_\infty)$ dropped to 1% of the inlet excess $(T_{in} - T_\infty)$, as opposed to the other investigations discussed above where the zero vertical velocity location is used. They obtained the following empirical scaling correlation for the fountain height,

$$z_m = 5.83 Fr^{0.88}. \tag{6}$$

Lin and Armfield [6] conducted numerical investigations to study the effect of the Reynolds number on the height of plane fountains. For $Re > 200$ they found that the fountain height is independent of the Reynolds number and

$$z_m \sim Fr^{4/3}, \tag{7}$$

where the symbol "$\sim$" denotes "scale to". For $Re \leq 200$ the fountain height was found to be dependent on the Reynolds number with the following analytical scaling

$$z_m \sim Fr Re^{-1/2}. \tag{8}$$

The scaling equation (8) was then confirmed by a series of numerical investigations [7] for $0.2 \leq Fr \leq 1.0$, $5 \leq Re \leq 500$ and $Pr = 7$ and they obtained the following relations

$$z_m = 0.2774 + 1.8696\, Fr, \tag{9}$$

$$z_m = 1.891 + 3.671\, Re^{-\frac{1}{2}}. \tag{10}$$

As shown above similar scaling relations have been obtained by various researchers, however there are significant variations in the constant of proportionality [8].

In this study, we investigate the influence of the Froude number on plane fountains and obtain empirical relations between the height and the Froude number for $50 \leq Re \leq 150$ and $0.25 \leq Fr \leq 10$. The effect of Prandtl number on fountain height is studied for Pr=7, 300 and 700 on two Froude numbers Fr=1.0 and Fr=2.0. Additionally we obtain the critical Froude number for a flapping instability.

Numerical method

The fluid between horizontal insulated solid walls a distance H apart is initially still and isothermal at temperature T_∞. For $t > 0$ fluid issues from a slot of width $2X_{in}$ in the floor with a parabolic velocity profile

$$V = V_m \left[1 - \left(\frac{X}{X_{in}}\right)^2\right], \tag{11}$$

where V_m is the maximum velocity of the parabolic profile which is equal to $1.5V_{in}$ for a fully developed laminar flow and temperature $T_{in} < T_\infty$. The flow is assumed to remain two-dimensional. Figure 1 shows the computational domain. The buoyancy is a result of the temperature difference between the source and the ambient fluids.

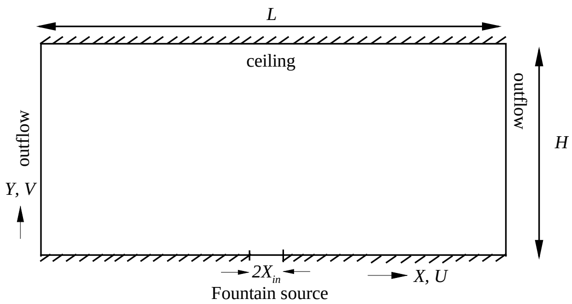

Figure 1: Computational domain.

The governing equations are the incompressible Navier–Stokes equations with the Oberbeck–Boussinesq approximation. The following equations are written in conservative, non-dimensional form in Cartesian coordinates,

$$\frac{\partial u}{\partial x} + \frac{\partial v}{\partial y} = 0\,, \tag{12}$$

$$\frac{\partial u}{\partial \tau} + \frac{\partial (uu)}{\partial x} + \frac{\partial (vu)}{\partial y} = -\frac{\partial p}{\partial x} + \frac{1}{Re}\left(\frac{\partial^2 u}{\partial x^2} + \frac{\partial^2 u}{\partial y^2}\right), \tag{13}$$

$$\frac{\partial v}{\partial \tau} + \frac{\partial (uv)}{\partial x} + \frac{\partial (vv)}{\partial y} = -\frac{\partial p}{\partial y} + \frac{1}{Re}\left(\frac{\partial^2 v}{\partial x^2} + \frac{\partial^2 v}{\partial y^2}\right) + \frac{1}{Fr^2}\theta, \tag{14}$$

$$\frac{\partial \theta}{\partial \tau} + \frac{\partial (u\theta)}{\partial x} + \frac{\partial (v\theta)}{\partial y} = \frac{1}{RePr}\left(\frac{\partial^2 \theta}{\partial x^2} + \frac{\partial^2 \theta}{\partial y^2}\right). \tag{15}$$

The following non-dimensionalisation is used:

$$x = \frac{X}{X_{in}},\ y = \frac{Y}{X_{in}},\ u = \frac{U}{V_{in}},\ v = \frac{V}{V_{in}},$$
$$\tau = \frac{t}{(X_{in}/V_{in})},\ p = \frac{P}{\rho V_{in}^2},\ \theta = \frac{T - T_\infty}{T_\infty - T_{in}}. \tag{16}$$

The initial and boundary conditions are

$$u = v = \theta = 0 \text{ when } \tau < 0, \tag{17}$$

and when $\tau \geq 0$

$$\frac{\partial u}{\partial x} = 0,\ \frac{\partial v}{\partial x} = 0,\ \frac{\partial \theta}{\partial x} = 0 \text{ on } x = \pm L/(2X_{in}), \tag{18}$$

$$u = 0,\ v = 1.5(1 - x^2),\ \theta = -1 \quad \text{on } |x| \le 1,\ y = 0\,, \tag{19}$$

$$u = v = 0,\ \frac{\partial \theta}{\partial y} = 0 \text{ on } |x| > 1,\ y = 0\ , \tag{20}$$

$$u = v = 0,\ \frac{\partial \theta}{\partial y} = 0 \text{ on } \quad y \quad = H/X_{in}, \tag{21}$$

respectively.

The results were obtained using the open source code Gerris [9], a quad-tree based adaptive mesh solver which uses a fractional-step projection method. The advective terms are discretised using a second-order Godunov type scheme, the remaining terms use standard second-order schemes and the equations are solved using a semi-implicit multi-grid approach. The computational domain is $-100 \le x \le +100$ and $0 \le y \le 100$. The minimum grid spacing is 4.88×10^{-4} in each direction. The mesh is dynamically adapted based on the vorticity and the temperature. The adaptive refinement is performed at the fractional timestep. A cell is refined, i.e. divided into four square sub-cells, whenever

$$\frac{|\nabla \times v|\, \Delta x}{\max |v|} \quad > \quad \delta, \tag{22}$$

$$|\nabla \theta|\, \Delta x \quad > \quad \delta. \tag{23}$$

where Δx is the size of the cell and δ is a user-defined threshold. The cells are also coarsened likewise. The code has been tested for different values of δ and CFL number. δ=0.01 and CFL=0.5 are found to be most appropriate and have been used throughout in the numerical calculations. The time-step varies dynamically during the iteration process. The time taken for a single run of $\tau = 1500$ on a typical Pentium-IV machine with 1GB RAM and 3.2GHz processor is 29 hours, although this time depends on the number of cells and thus varies with Froude number.

Fountain height scaling

In order to obtain the fountain height scaling it is assumed that Z_m can be expressed in terms of powers of the momentum flux m_{in}, the buoyancy flux b_{in} and the viscosity ν such that the power relation is as follow,

$$Z_m \sim m_{in}^{\alpha} b_{in}^{\beta} \nu^{\gamma}. \tag{24}$$

Dimensional analysis is then used to obtain the values of the powers. However we end up with a set of equations where there are only two dimensions, length and time and three unknown powers, α, β and γ. Thus we obtain one linearly independent solution. The dimensional analysis thus leads to the relation,

$$Z_m = X_{in} Fr^{\frac{4}{3} - \frac{2}{3}\gamma} Re^{-\gamma}. \tag{25}$$

In non-dimensional form equation (25) becomes,

$$z_m = \frac{Z_m}{X_{in}} \sim Fr^{\frac{4}{3} - \frac{2}{3}\gamma} Re^{-\gamma}. \tag{26}$$

For large Reynolds number, the fountain height will be independent of the viscosity and thus γ=0. The equation (26) then reduces to

$$z_m \sim Fr^{\frac{4}{3}}, \tag{27}$$

which is exactly same as equation (3) obtained by Baines et al. [1] for turbulent plane fountains. However in the present case, the power γ is unknown and will be evaluated empirically. Lin and Armfield [6] gave an analytical value for γ in case of weak fountains ($Fr \le 1.0$) by assuming that for low Reynolds number flow the height of the weak fountains is controlled by the rate at which fluid can exit the fountain via the viscous intrusion that forms downstream of the fountain. Lin and Armfield [6] obtained $\gamma = \frac{1}{2}$ and thus for weak fountains equation (26) becomes,

$$z_m \sim \frac{Fr}{Re^{\frac{1}{2}}}\,. \tag{28}$$

Results

The free-fountain results have been obtained with Reynolds numbers ranging from $50 \le Re \le 150$ for $0.25 \le Fr \le 10.0$. The effect of Prandtl number on fountain height is also examined for Pr=7, 300 and 700.

Observations

An overview of the temperature fields at different times for Fr=1.0 and Fr=1.25 at Re=100 and Pr=7 is shown in figure 2. After the fountain is initiated, it travels upwards until momentum balances buoyancy, when it comes to rest. The rising fluid spreads due to its reduced velocity and interaction with the ambient fluid. The descending fluid then interacts with the environment and with the upflow, restricting the rise of further fluid. The descending fluid, heavier than the ambient, moves along the floor as a gravity current. The fountain is symmetric and steady for Fr=1.0 at full development whereas the fountain starts symmetrically for Fr=1.25, but eventually becomes unsteady and asymmetric. An interesting feature is the flapping, i.e. lateral oscillation, that can be observed for Fr=1.25 in figure 2. The flapping phenomenon can be thought of as a lateral movement of the fountain fluid on either side of the fountain source. At the extreme of each oscillation the top of the fountain is shed laterally exposing the core of the fountain. The fountain then increases in height and the process is again repeated on the other side. This flapping behaviour can again be either periodic or aperiodic depending upon on the Froude number, which will be discussed later in this section.

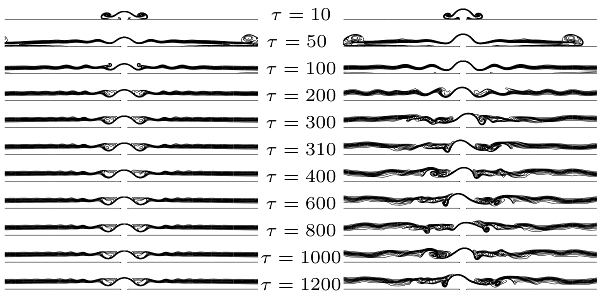

Figure 2: Evolution of temperature fields for Fr = 1.0 (left column) and Fr = 1.25 (right column) at Re=100 and Pr=7.

Figure 3 shows the instantaneous temperature fields for different Froude numbers. The fountain is observed to be steady and symmetric for Fr=1.0, but is asymmetric for all the higher Froude numbers ($Fr \ge 1.25$). The

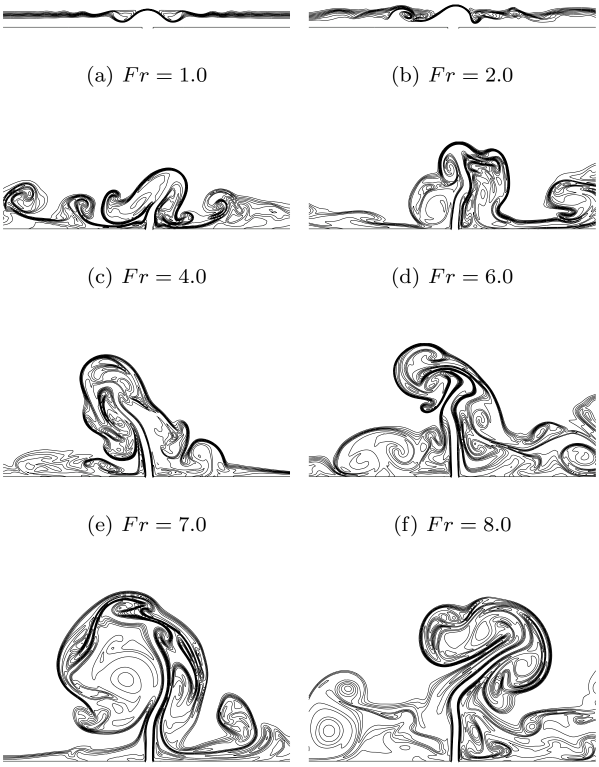

(a) $Fr = 1.0$ (b) $Fr = 2.0$

(c) $Fr = 4.0$ (d) $Fr = 6.0$

(e) $Fr = 7.0$ (f) $Fr = 8.0$

(g) $Fr = 9.0$ (h) $Fr = 10.0$

Figure 3: Instantaneous temperature fields after the flow is fully developed at Re=100 and Pr=7.

fountain also appears to be more chaotic as the Froude number increases.

This effect of the Froude number on the fountain is examined further in figure 4 which shows the time-evolution of u at x=0 and y=2. The horizontal velocity is almost zero with time for Fr=0.8 and 1.0, as shown in figure 4a, indicating that the fountain is symmetric about x=0. However, the fountain becomes asymmetric and flaps with a definite frequency, periodically, as shown in figures 4b–4d for Fr=1.25, 1.5, 2.0, and quasi-periodically for Fr=2.25 as shown in figure 4e. At Fr=2.5 the time-series is aperiodic, as shown in figure 4f and the same is true for all the higher Froude numbers (not shown).

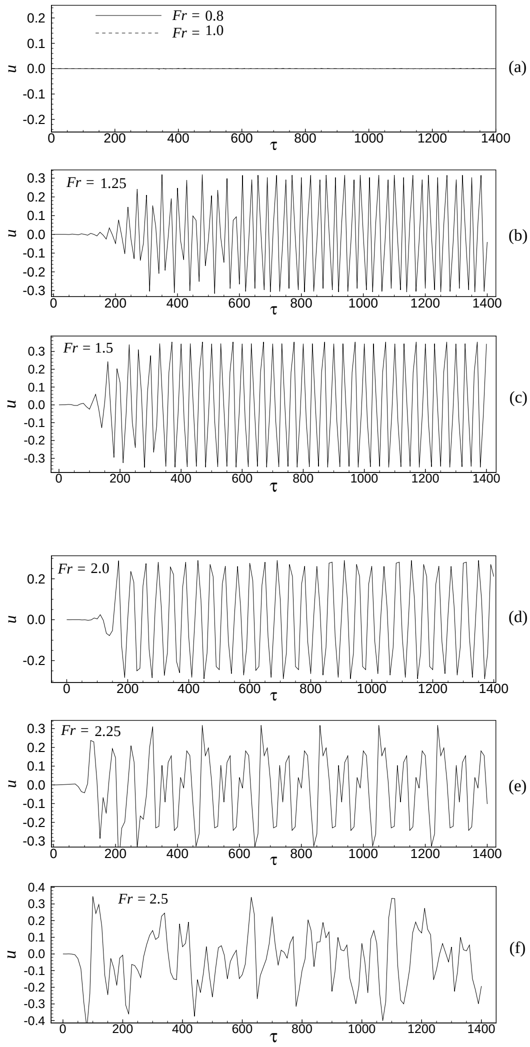

Figure 4: Evolution of u at $x = 0$ and $y = 2$ for different Froude numbers at Re=100 and Pr=7.

Effect of Reynolds number on Fountain height

The effect of the Reynolds number on the non-dimensional fountain height z_m is shown in figure 5. The results were obtained for Re=50, 75, 100, 125, 140 and 150 with Pr=7 and Fr=0.5, 2.0 and 6.0. The fountain height is measured as the vertical distance from fountain source to the point where the vertical velocity goes to zero. For unsteady and asymmetric fountains ($Fr \geq 1.25$), the fountain height is obtained as a time-average over τ=200–1400 and for lower Fr is the steady-state height. In the case of weak fountains ($Fr \leq 1.0$) where the fountains are steady and symmetric, it is found that increase in Reynolds number leads to a decrease in the fountain height. For weak fountains the steady-state fountain height provides the required energy to drive the fountain laterally outwards. As the viscosity of the fluid increases (decrease in Reynolds number) there is resistance to this outflow and thus more energy is required to drive the flow. This energy is obtained only by increasing the steady-state rise height of the fountain and thus for low Re flow the fountain height is higher.

In the case of fountains with intermediate (Fr=2.0) and large (Fr=6.0) Froude number where the fountains are unsteady and flap periodically and aperiodically respectively, an increase in Reynolds number increases the fountain height. For such flow there is still enough energy (higher momentum flux compared to buoyancy flux) even at low Reynolds number to overcome any resistance to the outflow and thus fountain height increases with Re.

The scaling of fountain height with Re for each of the Fr considered (Fr=0.5, 2.0 and 6.0) is obtained empirically and as follows; in the steady and symmetric regime,

$$z_m = 1.19 + 6.64Re^{-0.5} \quad (29)$$

with a variation of less than ±0.004; in the unsteady and periodic flapping regime,

$$z_m = 4.4Re^{0.1} \quad (30)$$

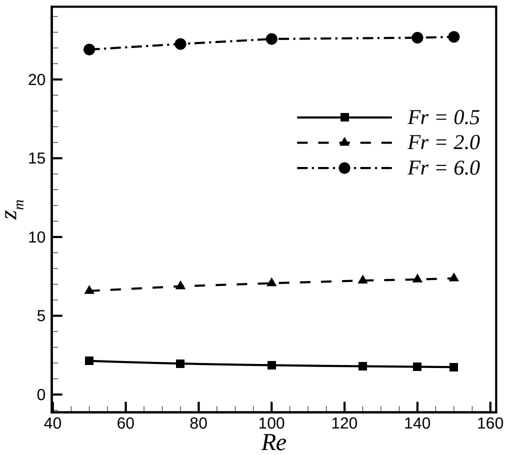

Figure 5: Variation of fountain height with Re for Fr=0.5, 2.0 and 6.0 at Pr=7.

with a variation of less than ±0.04; and in the unsteady and aperiodic flapping regime,

$$z_m = 19.25Re^{0.035} \tag{31}$$

with a variation of less than ±0.025.

The scaling equation (29) is similar to the result obtained by Lin and Armfield [6] for weak fountains. Not enough evidence is available in the literature on plane fountains to confirm the scalings given by equations (30) and (31). The scaling relations (equations (29)–(31)) thus give γ in equation (26) as 0.5, -0.1 and -0.035 for Fr=0.5, 2.0 and 6.0 respectively. Thus $|\gamma|$ gradually decreases with increase in Fr, showing there is rather a weak dependence of fountain height on Reynolds number for larger Fr.

Effect of Prandtl number on Fountain height

The effect of Prandtl number on fountain height is studied for Pr=7, 300 and 700 with two Froude numbers namely Fr=1.0 and Fr=2.0 at Re=100. Figure 6 shows the variation of z_m with Pr for this range. The variation

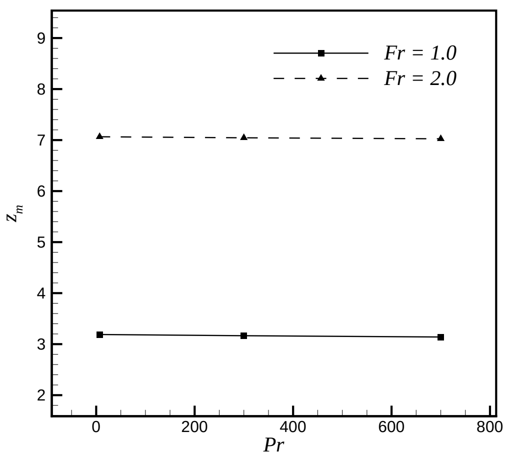

Figure 6: Variation of fountain height with Pr for Fr=1.0 and 2.0 at Re=100.

is negligible and thus it can be concluded that z_m does not vary with Pr over this range. This result agrees well with the analytical scaling relation (equation 26) where z_m is independent of Pr.

Effect of Froude number on Fountain height

The variation of fountain height with Froude number is shown in figure 7 for Re=50, 100 and 150 at Pr=7. Since

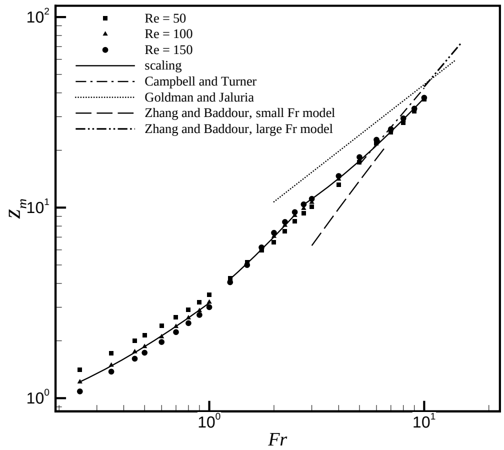

Figure 7: Variation of fountain height with Fr for Re=50, 100 and 150 at Pr=7.

three different regimes in the fountain were identified and the fountain height scales differently with Reynolds for each of the regimes, it is appropriate to use three different fountain height scalings with Fr. A comparison of results with those obtained by previous researchers is also shown in figure 7. Most of the experimental results available on plane fountains are for intermediate and high Fr ($Fr \geq 3.0$) in transitional and turbulent regimes. Lin and Armfield [6, 7] have obtained numerical results for weak fountains.

The results show that the fountain height increases with Fr in all the regimes. For weak fountain ($Fr \leq 1.0$) the fountain height decreased with Re which has been discussed previously. Although figure 7 shows data for Re=50, 100 and 150, the fit (solid line in figure 7) is obtained for a fixed Reynolds number of Re=100. All scaling relations are obtained and plotted based on the constant γ obtained from equations (29)–(31) and using the scaling relation from equation (26). In the steady and symmetric region ($0.25 \leq Fr \leq 1.0$)

$$z_m = 0.571 + 2.586Fr \tag{32}$$

with a variation of less than ±0.011. In the periodic and quasi-periodic flapping region ($1.25 \leq Fr \leq 2.25$),

$$z_m = 1.2108 + 2.2016Fr^{1.4} \tag{33}$$

with a variation of less than ±0.022. In the unsteady and aperiodic flapping region ($2.5 \leq Fr \leq 10.0$),

$$z_m = 4.45 + 1.536Fr^{4/3} \tag{34}$$

with a variation of less than ±0.37.

Discussion and conclusions

The long-term transient behaviour of plane fountains, with parabolic inlet velocity profiles, has been studied numerically for $50 \leq Re \leq 150$, $0.25 \leq Fr \leq 10.0$ and Pr=7, 300, 700. Three distinct regimes have been identified. In the first regime, the fountain is symmetric and steady with Froude number varying from $0.25 \leq Fr \leq 1.0$. Similar flow patterns were observed by Lin and Armfield [7] with weak laminar plane fountains ($0.2 \leq Fr \leq 1.0$). In the second regime ($1.25 \leq Fr \leq 2.25$), the fountain is unsteady and asymmetric but has a periodic flapping. In the third regime ($Fr \geq 2.5$), the fountain is unsteady and aperiodic. The critical Froude number for transition from steady to unsteady flow lies between $Fr = 1.0$ and 1.25.

The periodic and quasi-periodic flapping behaviour observed here has not been reported previously. However most of the work carried out by previous researchers was in the intermediate and large Fr range ($Fr \geq 3.0$), at higher Fr than those at which the periodic and quasi-periodic flapping has been observed. Additionally most of the previous experimental work has used a re-entrant nozzle, whereas we have used fountain source flush with the floor. Initial results with a re-entrant nozzle at Fr=2.0 (not shown here) showed a strongly asymmetric flow with no flapping, and it may be that periodic and quasi-periodic flapping behaviour is only generated with a source flush with the floor. Lin and Armfield [6, 7] did use a source flush with the floor, but with $Fr \leq 1.0$ considered only flows for which flapping is not expected. A number of researchers have observed aperiodic flapping and chaotic unsteady flows at higher Fr, similar to those observed here for $Fr \geq 2.5$ [1, 2, 3].

The scaling relations between the fountain height and the Reynolds number at the source have been obtained empirically for Fr=0.5, 2.0 and 6.0 with a fixed Prandtl number of Pr=7 for Re=50, 75, 100, 125, 140 and 150. The fountain height decreases with increase in Reynolds number for steady and symmetric fountains but increases with Reynolds number for unsteady fountains. In the steady and symmetric regime, $z_m \sim Re^{-\frac{1}{2}}$. In the periodic and quasi-periodic flapping regime, $z_m \sim Re^{0.1}$ and in the unsteady and aperiodic regime, $z_m \sim Re^{0.035}$. In the unsteady regime, as the Froude number increases the dependence of fountain height on Re decreases. Fountains with higher Fr are approaching turbulence and thus can be approximated with turbulent fountains where the fountain height is independent of Reynolds number.

The effect of Prandtl number on Froude number is also studied for a fixed Re of 100 with Fr=1.0 and 2.0 for Pr=7, 300 and 700. It is found that the fountain height does not vary with Pr in this range.

In addition the scaling of fountain height with Fr is obtained for $0.25 \leq Fr \leq 10.0$ with Re=100 and Pr=7. It is found that the fountain height increases with Fr in all the regimes. In the steady and symmetric regime ($0.25 \leq Fr \leq 1.0$), $z_m \sim Fr$ is obtained from the analytical scaling and provides a good representation of the behaviour in this regime. This result agrees well with the analytical scaling obtained by Lin and Armfield [7] with a small variation in the constant possible as a result of the different boundary condition and integration times used there. In the periodic and quasi-periodic regime ($1.25 \leq Fr \leq 2.25$) a best fit to the data gave $z_m \sim Fr^{1.4}$, no analytical scaling or other results are available to furthur validate this. In the aperiodic, chaotic regime ($2.5 \leq Fr \leq 10.0$) the analytical relation $z_m \sim Fr^{4/3}$ [1] is found to provide a good fit, with negligible Re variation, in good agreement with the results of Campbell and Turner with C=1.97 [2] and with the large Fr results of Zhang and Baddour [3]. Both the small Fr virtual source model of Zhang and Baddour and the Goldman and Jaluria model [5] provide poor prediction of the data obtained here. In the latter case this may be due to the experimental set up and different definition of the fountain height, while Zhang and Baddour small Fr model is not applicable to the full Fr range considered.

The current authors have also conducted experiments and limited three-dimensional numerical simulations (due to computational limitations) on both planar and round fountains with a flush source. There is a good agreement between experiments and numerical results quantitatively over the range of Fr and Re considered in this paper. Further, the flapping mode described in this paper is also observed in experiments for both planar and round fountains. The scaling relations are yet to be confirmed for three-dimensional fountains and it is expected that current scaling relations will hold good with some variations in the constant of proportionality.

Acknowledgments

The support of the Australian Research Council is gratefully acknowledged.

References

[1] W. D. Baines, J. S. Turner, I. H. Campbell, Turbulent fountains in an open chamber, *J. Fluid Mech.*, **212**, 1990, 557–592.

[2] I. H. Campbell, J. S. Turner, Fountains in magma chambers, *J. Petrol*, **30**, 1989, 885–923.

[3] H. Zhang, R. E. Baddour, Maximum vertical penetration of plane turbulent negatively buoyant jets, *J. Eng. Mech.*, **123**, 1997, 973–977.

[4] B. R. Morton, Forced Plumes, *J. Fluid Mech.*, **5**, 1959, 151–163.

[5] D. Goldman, Y. Jaluria, Effect of opposing buoyancy on the flow in free and wall jets, *J. Fluid Mech.*, **166**, 1986, 41–56.

[6] W. Lin, S. W. Armfield, The Reynolds and Prandtl number dependence of weak fountains, *Computational Mech.*, **31**, 2003, 379–389.

[7] W. Lin, S. W. Armfield, Direct simulation of weak laminar plane fountains in a homogeneous fluid, *Int. J. Heat Mass Transfer*, **43**, 2000, 3013–3026.

[8] E. J. List, Turbulent jets and plumes, *Ann. Rev. Fluid Mech.*, **14**, 1982, 189–212.

[9] S. Popinet, Gerris: a tree-based adaptive solver for the incompressible Euler equations in complex geometries, *J. Comput. Phys.*, **190**, 2003, 572–600.